5. M. Rubenstein and P. J. Dean, *J. Appl. Phys.*, **41**, 1777 (1970).
6. G. A. Silvey, *ibid.*, **29**, 226 (1958).
7. W. J. Turner, A. S. Fischler, and W. E. Reese, *Phys. Rev.*, **121**, 759 (1961).
8. G. A. Silvey, V. J. Lyons, and V. J. Silvestri, *This Journal*, **108**, 653 (1961).
9. A. S. Jordan, *This Journal*, **118**, 781 (1971).
10. A. N. Nesmeyanov, B. Z. Iofa, A. A. Strelnikov, and V. G. Fursov, *Zhur. Fiz. Khim.*, **30**, 1250 (1956).
11. V. J. Lyons and V. J. Silvestri, *J. Phys. Chem.*, **64**, 266 (1960).
12. J. B. Westmore, K. H. Mann, and A. W. Tickner, *ibid.*, **68**, 606 (1964).
13. R. C. Schoonmaker, A. R. Venkitaranan, and P. K. Lee, *ibid.*, **71**, 2676 (1967).
14. R. C. Schoonmaker and K. Rubinson, *ibid.*, **71**, 3354 (1967).
15. C. L. McCabe, *J. Metals*, **6**, 969 (1954).
16. P. Goldfinger and M. Jeunehomme, *Trans. Faraday Soc.*, **59**, 2851 (1963).
17. D. R. Stull and G. C. Sinke, "Thermodynamic Properties of the Elements," Advances in Chemistry Series, No. 18, Am. Chem. Soc.
18. S. M. Ariya, M. P. Morozova, Khuan Tszi-tao, and E. Volf, *J. Gen. Chem. U.S.S.R.*, **27**, 325 (1957).
19. K. K. Kelley, U.S. Bur. of Mines Bull. 584 (1960); and K. K. Kelley and E. G. King, U.S. Bur. of Mines Bull. 592 (1961), U.S. Govt. Printing Office, Washington, D.C.
20. N. N. Sirota and E. M. Smolyarenko, in "Chemical Bonds in Semiconductors and Thermodynamics," Consultants Bureau (Plenum Publishing Corp.), New York (1968).
21. V. J. Lyons, *J. Phys. Chem.*, **63**, 1142 (1959).
22. I. J. Hegyi, E. E. Loebner, E. N. Poor, Jr., and J. G. White, *J. Phys. Chem. Solids*, **24**, 333 (1963).
23. A. Jayaraman, T. R. Ananthraman, and W. Klement, Jr., *ibid.*, **27**, 1605 (1966).
24. V. M. Glazov and M. Kasymova, *Proc. Acad. Sci. U.S.S.R. (Dokl.), Phys. Chem. Sect.*, **183**, 803 (1968).
25. O. Kubaschewski, E. LL. Evans, and C. B. Alcock, "Metallurgical Thermochemistry," 4th Ed., Pergamon Press Ltd. (1967).
26. JANAF, Thermochemical Tables, Thermal Labs., Dow Chemical Co.
27. M. Hansen, "Constitution of Binary Alloys," McGraw-Hill Book Co., Inc., New York (1958).
28. D. Lichter and P. Sommelet, *Trans. Met. Soc. AIME*, **245**, 99 (1969).
29. C. D. Thurmond, *J. Phys. Chem. Solids*, **26**, 785 (1965).
30. "Selected Values of Chemical Thermodynamic Properties," NBS Technical Note 270-3, Washington, D.C. (1968).
31. J. R. Arthur, *J. Phys. Chem. Solids*, **28**, 2257 (1967).
32. W. Schottky and M. B. Bever, *Acta Met.*, **6**, 320 (1958).
33. P. M. Robinson and M. B. Bever, in "Intermetallic Compounds," J. H. Westbrook, Editor, John Wiley & Sons, Inc., New York (1967).
34. A. S. Jordan and R. R. Zupp, *This Journal*, **116**, 1264 (1969).

Vaporization in the PbTe-SnTe System[1]

David A. Northrop

Sandia Laboratories, Albuquerque, New Mexico 87115

ABSTRACT

The vaporization of three alloys in the PbTe-SnTe system has been investigated thermogravimetrically. The vaporization is noncongruent as SnTe, the more volatile component, is lost preferentially. Due to the similarity of the PbTe and SnTe vapor pressures, the observed differences in total effusion rates between the alloys and changes in rate expected due to noncongruency are of the magnitude of the experimental error and the vaporization appears to be congruent in gravimetric experiments. Effusion rates, composition changes, and approximate vapor pressures have been determined with the results falling between the limits given by PbTe and SnTe. The results for a commercial, (Pb,Sn)Te thermoelement are given for comparison with this work and previously published investigations.

Vaporization of alloys in the PbTe-SnTe system has been investigated as part of a continuing study of vaporization in the (Pb,Sn,Ge)Te system (1). Considerable interest has been shown in the PbTe-SnTe pseudobinary system as these alloy compositions are in use as the p-junction in several isotope power generator systems. The vaporization of three compositions was studied: $Pb_{0.91}Sn_{0.09}Te$, $Pb_{0.72}Sn_{0.28}Te$, and $Pb_{0.50}Sn_{0.50}Te$. In addition, the results for a commercial, p-type thermoelement are given which were obtained with the same effusion cells and procedures so that a direct comparison could be made.

Commercial p-type thermoelements of nominal $Pb_{0.50}Sn_{0.50}Te$ composition were used for the free surface vaporization rates given by Bates and Weinstein (2), and in the mass spectrometric effusion studies by Winchell (3). The latter investigator concluded that the vaporization was either congruent or "pseudocongruent" and occurs by the loss of SnTe and PbTe molecules in the same relative concentrations as in the solid. Sokolov *et al.* (4), on the other hand, found a SnTe-rich vapor over a $Pb_{0.52}Sn_{0.48}Te$ material, which would indicate noncongruency and a progressively Pb-enriched alloy composition. These studies are discussed in more detail later in this report.

Other studies in the PbTe-SnTe system have been concerned with determination of the phase relations (5-8), examination of the variation of lattice parameter with composition (5-7, 9-12), growth and characterization of single crystals (7, 8, 13), and investigation of electrical properties (6-8, 14, 15). The over-all results show that PbTe and SnTe form a complete range of solid solutions which exhibit nearly ideal behavior. The temperature-composition phase relations are in the shape of a simple lens with end points given by the melting points of 917° and 806°C for pure PbTe and SnTe, respectively, and a maximum difference between the liquidus and solidus of ~18°C at 45 m/o (mole per cent) SnTe (5). Lattice parameters show slight positive deviations from Vegard's law when the exact tellurium concentration is considered. The single-phase (Pb,Sn)Te compositions are all p-type and thus the field lies on the Te-rich side of the PbTe-

[1] This work was supported by the U.S. Atomic Energy Commission.

Key words: lead telluride, tin telluride, vapor pressure, effusion, thermoelement.

SnTe binary join (13). The liquidus surface of the Pb-Sn-Te ternary system has also been determined (16).

Experimental Details and Results

General.—A detailed description of the apparatus, methods, and sources of error is given elsewhere (1), and only specific details are reported here. An automatic recording balance was used and its continuous weight, time, and temperature record is particularly suited for the investigation of noncongruent vaporizations where changing rates of loss are expected.

Three alloys were made from the elements (of stated purity > 99.99%) by reaction at 950°C in evacuated quartz ampoules. The ampoules were air quenched from this temperature, and the samples were reground finer than 240 mesh and annealed at 600°C for 48 hr, also in evacuated quartz ampoules. The lead concentration was determined by polarography and the alloy composition was calculated assuming an exact $Pb_xSn_{1-x}Te$ stoichiometry. The initial alloy compositions are, to ±0.01 a/o (atomic per cent), $Pb_{0.91}Sn_{0.09}Te$, $Pb_{0.72}Sn_{0.28}Te$, and $Pb_{0.50}Sn_{0.50}Te$. Powder x-ray diffraction analyses indicated that only the alloy phase was present.

Graphite and alumina effusion cells were used, and their effective orifice areas were determined by effusion of a lead standard (1). Three types of effusion experiments were made: Type 1: Isothermal runs in which ~80 mg were effused until a constant cell weight was observed. Type 2: isothermal runs which were quenched at successive stages of vaporization and samples taken for x-ray and polarographic analyses. The initial amount of sample was ~1200 mg and two cuts and a final residue were obtained for each run. For each cut, the sample was removed from the cell, reground and mixed thoroughly, ~100 mg removed permanently for analysis, and the remainder replaced in the cell for further vaporization. Type 3: effusion runs of ~20 rate-temperature data points for the vapor pressure calculations. The initial sample weight was 800-900 mg and no more than a third was vaporized in a single run.

Vapor species.—No direct determination of the vapor species was made in this investigation. It is assumed that (Pb,Sn)Te vaporizes by the loss of molecular SnTe(g) and PbTe(g), and this assumption is based on the results for the pure end members and the following reported mass spectrometric data for the alloys. Winchell (3) observed approximately equal intensities of $SnTe^+$ and $PbTe^+$ but no Te_2^+ or higher molecular weight ions for a thermoelement of approximate composition $Pb_{0.5}Sn_{0.5}Te$. Sokolov *et al.* (4) examined the effusion of a $Pb_{0.52}Sn_{0.48}Te$ sample at 760°C and identified the following parent ions with relative intensities given in parentheses: $SnTe^+$ (132), $PbTe^+$ (100), Te_2^+ (~1), $SnTe_2^+$ (~1), and lesser amounts of $Sn_2Te_2^+$, $PbSnTe_2^+$, and $PbSnTe^+$. Unambiguous determination of the equilibrium vapor is hindered by electron impact dissociation in the mass spectrometer ion source, and atomic ions produced by fragmentation were observed in both studies.

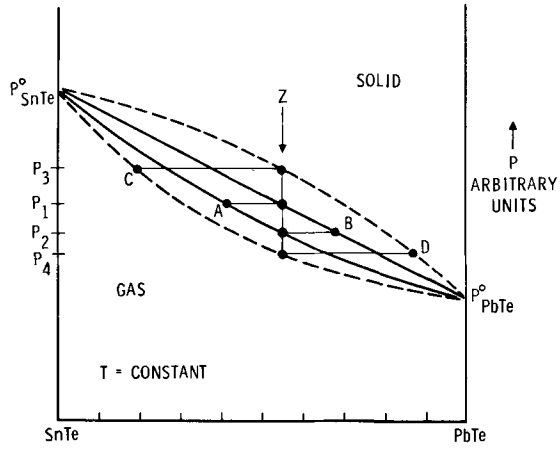

Fig. 1. Possible pressure-composition phase relations for the PbTe-SnTe system showing the compositional relations for the ideal (solid lines) and a typical nonideal (dashed lines) solid solution.

Congruency.—A noncongruent vaporization of (Pb,Sn)Te alloys was expected and was confirmed by several experiments. The prediction was made by examination of the schematic pressure-composition phase relations shown in Fig. 1 for a binary alloy system exhibiting a complete range of solid solutions. In addition, while PbTe vaporizes congruently, SnTe vaporizes noncongruently with the loss of a slight excess of Te which first produces a two-phase, Sn-SnTe assemblage, and then a very small amount of pure Sn as a final phase (1). Thus noncongruency has to be examined from two standpoints: the relative loss of SnTe with respect to PbTe and also the possibility of the formation of a metal second phase.

The results for the type 2 effusion runs are given in Table I. Each cut was analyzed polarographically for total lead content and an alloy composition was calculated on the assumption that only a stoichiometric $Pb_xSn_{1-x}Te$ phase was present. The results are semiquantitative with the uncertainty arising from both the analytical technique and possible inhomogeneities and minor phases present in the cut. Each alloy was investigated at 625°, 700°, and 825°C, but the three results were averaged in each case as no general temperature dependence could be observed.

A small portion of each cut (<1 mg) was examined by x-ray diffraction utilizing the Debye-Scherrer technique and Ni-filtered, CuKα radiation. From published reports (9), the alloy lattice constant can be related to its composition provided that the exact Te stoichiometry is known from the carrier concentration or other measurements. The lack of this information and the uncertainty that such a small portion of the total sample would accurately reflect the bulk composition precluded any quantitative analysis by x-ray methods. Qualitatively, however, comparative line shifts in the back-reflection region indicated that in every case the observed *d*-spacings became greater (increased PbTe concentration) with increased vaporization.

Table I. Alloy composition as a function of amount vaporized

Material	Initial composition	Cut A		Cut B		Residue	
		Amt lost, w/o	Composition	Amt lost, w/o	Composition	Amt lost, w/o	Composition
Type 2 effusion runs:							
$Pb_{0.91}Sn_{0.09}Te$	91/09	18	94/06	39	96/04	59	99/01
$Pb_{0.72}Sn_{0.28}Te$	72/28	19	77/23	36	78/22	63	82/18
$Pb_{0.50}Zn_{0.50}Te$	50/50	22	54/46	48	58/42	75	64/36
Residue from the type 3 effusion runs:							
Curve 1, Fig. 2	91/09					22	92/08
	91/09					22	93/07
Curve 2, Fig. 2	72/28					24	78/22
	72/28					25	77/23
Curve 3, Fig. 2	50/50					32	52/48
	50/50					31	54/46

The residues from the type 3 effusion experiments were also analyzed by the two methods. The results are also given in Table I and the same trend is found.

The possibility of the formation of a metallic second phase is more difficult to assess. If the original stoichiometric concentrations of the elements were maintained, the initial alloys should be two-phase, (Pb,Sn) and (Pb,Sn)Te, as the single-phase alloy compositions lie on the Te-rich side of the PbTe-SnTe binary join (13). However, a metal second phase could not be detected in x-ray powder patterns of either the initial alloys or any cuts from the special effusion runs. Isothermal effusion runs (type 1) to constant weight with pure SnTe resulted in a Sn residue of ~0.3 w/o. Similar experiments with the $Pb_{0.50}Sn_{0.50}Te$ alloy produced a trace residue (<0.1 w/o) which was identified by x-ray diffraction as SnO_2, and its exact origin is unknown. Pb would not be expected in the residue at a constant observed weight as its vapor pressure is of the same order of magnitude as lead telluride. In the type 1 effusion runs, care was taken to insure that the cell temperature did not overshoot the intended run temperature. During the first 5 w/o of loss, the maximum observed rate decreased by ~7% to an essentially constant rate for the balance of the run. In the noncongruent vaporization of GeTe, this rate-time behavior was interpreted as the rapid loss of excess Te to drive the over-all composition into a Ge-GeTe two-phase region (1). The same interpretation could be applied in this case, and further evidence is found in the parent Te_2^+ contribution reported by Sokolov *et al.* (4).

To summarize, the vaporization of (Pb,Sn)Te is noncongruent. The primary composition change is a decrease in the SnTe/PbTe ratio due to the preferential loss of SnTe(g). There is inconclusive evidence for the loss of additional tellurium but in amounts that should not affect the results and discussions in this report.

Effusion rates.—Two type 3 effusion runs were made with different graphite cells for each alloy. Unless assumptions are made concerning the relative vapor composition and its change due to noncongruency, the total vapor pressure cannot be calculated from the total rate of weight loss as is usually done *via* the Knudsen equation

$$P_T = \sum_i P_i = \sum_i \left(\frac{1}{A}\right) x_i \left(\frac{dw}{dt}\right)_T \sqrt{\frac{2\pi RT}{M_i}} \quad [1]$$

where A is the effective orifice area, $(dw/dt)_T$ is the total observed rate of weight loss, and x_i and M_i are the weight fraction and molecular weight of the ith vapor species. Alternatively, a quantity Q_T has been defined

$$Q_T = \left(\frac{1}{A}\right)\left(\frac{dw}{dt}\right)_T \sqrt{2\pi RT} \quad [2]$$

which is essentially proportional to the observed effusion rate and is related to the total vapor pressure by

$$P_T = Q_T \sum_i x_i \sqrt{\frac{1}{M_i}} \quad [3]$$

The reason for presenting the data in terms of Q_T is to emphasize the similarity of the observed effusion rates for this alloy system.

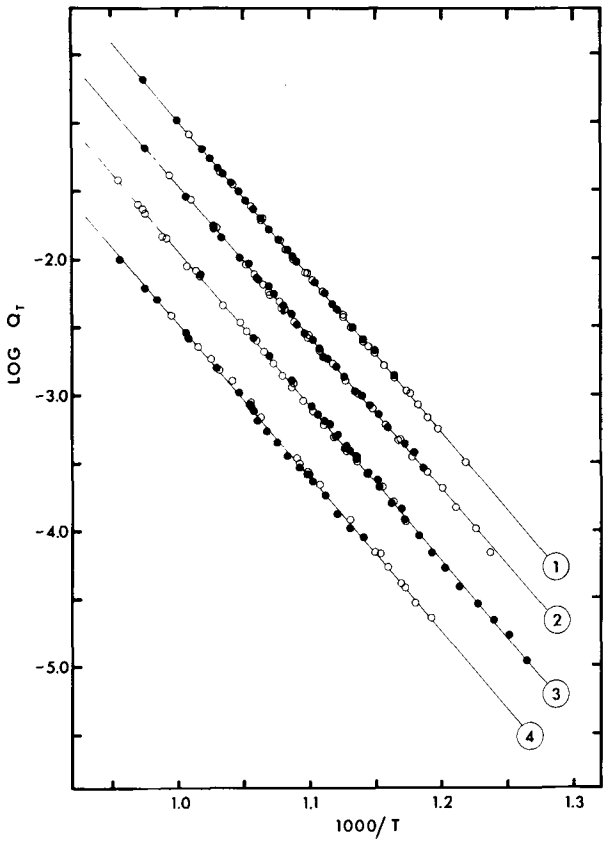

Fig. 2. Experimental data for the type 3 effusion runs expressed as log Q_T *vs.* reciprocal temperature: curve 1, $Pb_{0.91}Sn_{0.09}Te$; curve 2, $Pb_{0.72}Sn_{0.28}Te$; curve 3, $Pb_{0.50}Sn_{0.50}Te$; curve 4, thermoelement. Ordinate scale applies to curve 4; each of the other curves has been offset from the other by log Q_T = 0.50 for clarity.

If the summed term is relatively constant during an effusion run, as in the case of a large sample and small over-all weight change, then Q_T is directly proportional to P_T and a plot of log Q_T *vs.* reciprocal temperature should be essentially linear with a slope equal to the enthalpy of vaporization. Linear least-squares fit of log Q_T as a function of $1/T$ resulted in equations of the form

$$\log Q_T = (A \pm \sigma_A) + (B \pm \sigma_B)(1000/T) \quad [4]$$

where σ_i are the standard deviations associated with the constants. The results for the two effusion runs for each of the three alloys and the thermoelement are shown in Fig. 2 and summarized in Table II. Values of Q_T for PbTe and SnTe have been calculated from the average summary equation given in Tables III and V, respectively, of Ref. (1).

Steady state and equilibrium.—In these experiments, the effective orifice areas of the effusion cells ranged from 4.49 x 10^{-4} to 5.64 x 10^{-3} cm^2 and the sample was

Table II. Effusion results expressed in terms of log Q_T and the experimental enthalpy of vaporization

Material	Average temp (°C)	log $Q_T = A + B(1000/T)$ A	B	ΔH_{vap} (kcal/mole)
PbTe[1]	634	8.837 ± 0.058	−11.294 ± 0.177	51.68 ± 0.81
$Pb_{0.91}Sn_{0.09}Te$	640	9.026 ± 0.024	−11.506 ± 0.022	52 65 ± 0.10
$Pb_{0.72}Sn_{0.28}Te$	634	8.781 ± 0.038	−11.236 ± 0.035	51.42 ± 0.16
$Pb_{0.50}Sn_{0.50}Te$	634	8.989 ± 0.042	−11.426 ± 0.038	52.29 ± 0.17
SnTe[1]	635	8.972 ± 0.083	−11.360 ± 0.182	51.98 ± 0.83
Thermoelement	654	8.836 ± 0.071	−11.310 ± 0.065	51.75 ± 0.30

[1] Calculated from data given in Ref. (1).

Table III. Calculated values of log Q_T and specific effusion rates at 650°C

Material	log Q_T	Specific effusion rate (g/cm² sec)	σ[1]	$\sigma_{\%}$[2]
PbTe[3]	−3.394	5.89×10^{-4}	0.037	±9
$Pb_{0.91}Sn_{0.09}Te$	−3.435	5.36×10^{-4}	0.009	±2
$Pb_{0.72}Sn_{0.28}Te$	−3.388	5.97×10^{-4}	0.016	±4
$Pb_{0.50}Sn_{0.50}Te$	−3.385	6.01×10^{-4}	0.021	±5
SnTe[3]	−3.331	6.81×10^{-4}	0.045	±11
Thermoelement	−3.413	5.64×10^{-4}	0.024	±6

[1] σ is the standard error of the estimate of the linear least-squares fit of log Q_T *vs.* reciprocal temperature. σ applies to the log Q_T values shown.
[2] $\sigma_{\%}$ is σ expressed as a per cent difference between Q_{calc} and Q_{obs} and applies to the rates shown.
[3] Calculated from data given in Ref. (1).

always ground finer than 340 mesh (<75μ). The vaporization coefficients for PbTe and SnTe are greater than 0.2 (1) and the attainment of steady-state conditions is not hindered by a low α_v or a low sample surface area/orifice area ratio as discussed by Motzfeldt (17). The observed effusion rates for all compositions were essentially constant during the type 1 effusion runs to greater than a 99 w/o loss. The rates then broke essentially discontinuously to zero (a constant cell weight). Thus, as little as 1 mg of material was sufficient to produce steady-state conditions in the cell. Surface enrichment of the less volatile phase (PbTe in this case) would normally tend to hinder vaporization and the attainment of steady-state conditions and would increase the apparent activity and vapor pressure of this phase. The results of the type 1 effusion experiments and the similar vapor pressures of PbTe and SnTe show that such effects are not detectable in these gravimetric experiments. In addition, the observed effusion rates and calculated pressures appear to be independent of orifice area within the range given above and, thus, a case can be made that these results represent the equilibrium values.

Discussion

The alloy vaporization can be described in terms of the P-X phase relations given in Fig. 1, where the solid and dashed lines indicate the phase boundaries for an ideal and a typical nonideal solid solution, respectively. In the ideal case, the exact boundaries can be calculated from the solid composition and the vapor pressures of the pure end members since, by definition, $P_i = x_i P_i^{\circ}$. The initial equilibrium vapor composition over an alloy of composition Z is given by A at a total pressure of P_1. As vaporization proceeds, both the vapor and solid compositions shift toward the less volatile component with Z and B becoming the concentrations of vapor and solid as the last solid vaporizes. Note that the vapor is always rich in the more volatile component and has the initial alloy composition only at the end of vaporization. The equilibrium total pressure decreases from P_1 to P_2 in the course of the vaporization. The representative nonideal case shown indicates that greater compositional and pressure changes would be expected: C going to Z for the vapor, Z going to D for the solid, and P_3 decreasing to P_4.

Table III gives values of log Q_T and specific, total rates of weight loss (g/cm² sec) calculated at 650°C. The similarity in these values is striking and can perhaps explain why these alloys have been interpreted as vaporizing congruently or "pseudocongruently" (3). The rate-temperature effusion data gave no systematic changes in observed rate with total weight loss up to losses of ~30 w/o. Furthermore, in the type 1 effusion runs, a continuous, over-all decrease in rate could not be definitely identified for any of the alloy compositions outside of the small initial decrease described earlier in the congruency discussion.

Several factors combine to explain this apparent congruency in these gravimetric experiments, and the over-all result is that the expected decrease in rate due to noncongruency is less than the over-all precision of the experimental procedure. First, the standard error of the estimates between log Q_{calc} and log Q_{obs} range from 0.009 to 0.045 which correspond to uncertainties of approximately ±2 to ±11% in Q_T. These uncertainties in themselves practically cover the entire range of calculated values given in Table III. Second, the temperature can be controlled to ±½°C during the isothermal effusion runs, and a 1° temperature change varies the observed rate by ~2.5% at these values of ΔH and temperature. Finally, only small changes in observed total rate are expected due to the similar vapor pressures of SnTe and PbTe. At a given temperature, the relative effusion rates for pure SnTe and PbTe are given by

$$\frac{\left(\frac{dw}{dt}\right)_{SnTe}}{\left(\frac{dw}{dt}\right)_{PbTe}} = \frac{P^{\circ}_{SnTe}}{P^{\circ}_{PbTe}}\sqrt{\frac{M_{SnTe}}{M_{PbTe}}} \qquad [5]$$

This rate ratio has the values of 1.133 and 1.171 at 550° and 725°C, respectively. Thus, an approximate 15% decrease in rate would occur during a hypothetical effusion run in which the solid composition would change from SnTe to PbTe. It is clear from Fig. 1 that a considerably smaller decrease would be observed during the vaporization of a given alloy composition. This change during a complete isothermal effusion can be calculated exactly if it is assumed that the system behaves ideally. For a 50/50 m/o alloy at 700°C (where $P^{\circ}_{SnTe}/P^{\circ}_{PbTe} = 1.359$), the ratio of initial to final rate is 1.0222; this is a decrease of approximately 2%.

Table IV shows the maximum composition changes that can be expected for a complete equilibrium vaporization if the alloy system is ideal. In every case, the observed composition changes are greater, suggesting nonideality and phase relations similar to those given by the dashed lines in Fig. 1. The observed changes eliminate the possibility of a more complicated double-lens type of phase diagram in the composition range $Pb_{0.5}Sn_{0.5}Te$ to PbTe. However, the possibility of a pressure maxima and a congruently subliming indifferent point (18) at the SnTe-rich end of the phase diagram is still compatible with the data.

It is desirable to calculate apparent total vapor pressures from the experimental data. As the vapor composition is continuously changing and has not been measured directly at any point in these experiments, an arbitrary, "average" molecular weight has been selected for this calculation. The initial vapor composition for an ideal alloy (Table IV) was selected and

Table IV. Calculated and observed composition changes at 700°C

Material	Calculated for an ideal solid solution[1]		Observed solid composition (from Table I)
	Initial vapor composition	Final solid composition at end of a complete vaporization	
$Pb_{0.91}Sn_{0.09}Te$	88/12	93/07	99/01 after a 59 w/o loss
$Pb_{0.72}Sn_{0.28}Te$	65/35	78/22	82/18 after a 63 w/o loss
$Pb_{0.50}Sn_{0.50}Te$	42/58	58/42	64/36 after a 75 w/o loss

[1] $P^{\circ}_{SnTe}/P^{\circ}_{PbTe} = 1.359$ at 700°C.

Table V. Approximate total vapor pressures based on an arbitrary average molecular weight

Material	Selected vapor composition	Average molecular weight	Log $P_T = A + B(1000/T)$ A	B	Calculated pressure at 650°C (atm)	σ%[2]
PbTe[1]	—	—	7.575	−11.294	2.21×10^{-5}	±9
$Pb_{0.91}Sn_{0.09}Te$	88/12	324.2	7.771	−11.506	2.04×10^{-5}	±2
$Pb_{0.72}Sn_{0.28}Te$	65/35	303.8	7.540	−11.236	2.35×10^{-5}	±4
$Pb_{0.50}Sn_{0.50}Te$	42/58	283.5	7.763	−11.426	2.45×10^{-5}	±5
SnTe[1]	—	—	7.776	−11.360	2.97×10^{-5}	±11
Thermoelement	42/58	283.5	7.610	−11.310	2.30×10^{-5}	±6

[1] From Ref. (1).
[2] See Table III.

the total weight loss has been ascribed to a vapor with this average molecular weight. For this comparative calculation, the error introduced by the arbitrary choice of vapor composition and not treating the data rigorously by Eq. [1] is less than the over-all experimental uncertainty. The equations for log Q_T in Table II can then be converted to log P_T by the addition of log $(M^{-1/2})$ to the A term. The results are given in Table V and the total vapor pressure curves presented in Fig. 3. Pressures calculated at 650°C given in Table V show more clearly the relative total vapor pressures for these materials. While a variation of pressure with alloy composition is evident, these pressures are practically indistinguishable within the limits set by the pure PbTe and SnTe when the experimental uncertainties are considered. It should be emphasized that the observed effusion rates are even more similar (see Table III) than the pressure curves given in Fig. 3; the molecular weight in the pressure calculation produces much of the vertical separation.

Thermoelements

3P,[2] p-type thermoelements were used in the studies of Winchell (3) and Bates and Weinstein (4), and were examined for comparative purposes in this work. While the exact composition is proprietary, this p-type material contains PbTe, SnTe, and MnTe in approximately 47/47/06 m/o proportions. MnTe is less volatile than the other two tellurides and can be identified as a residue in both effusion and free surface vaporizations. However, its accumulation did not affect the effusion results as seen in Fig. 2, curve 4. As for the alloy compositions discussed in an earlier section, no systematic variation of rate with time or amount vaporized was observed. Winchell did not detect any form of Mn in the vapor during his investigation (3).

The results have been calculated and presented along with the "pure" alloy materials, and they are closest to those for the 72/28 and 50/50 compositions. The approximate vapor pressure curve is given in Fig. 4 relative to pure SnTe and PbTe and the previously reported results of Winchell (3), Bates and Weinstein (2), and Sokolov *et al.* (4). Thus, the near-equilibrium vaporization behavior of this complex material is determined by the behavior of the major constituent and is relatively unaffected by minor phases or dopants added to enhance its electrical properties. Unpublished data from this laboratory indicate that this is also true for 3N[3] and TAGS[4] thermoelements where the near-equilibrium vaporization behavior is essentially identical to that of the major phase, PbTe and GeTe, respectively.

[2] The 3M Company, St. Paul, Minnesota 55101.
[3] The 3M Company, St. Paul, Minnesota 55101.
[4] Isotopes, Incorporated, Timonium, Maryland.

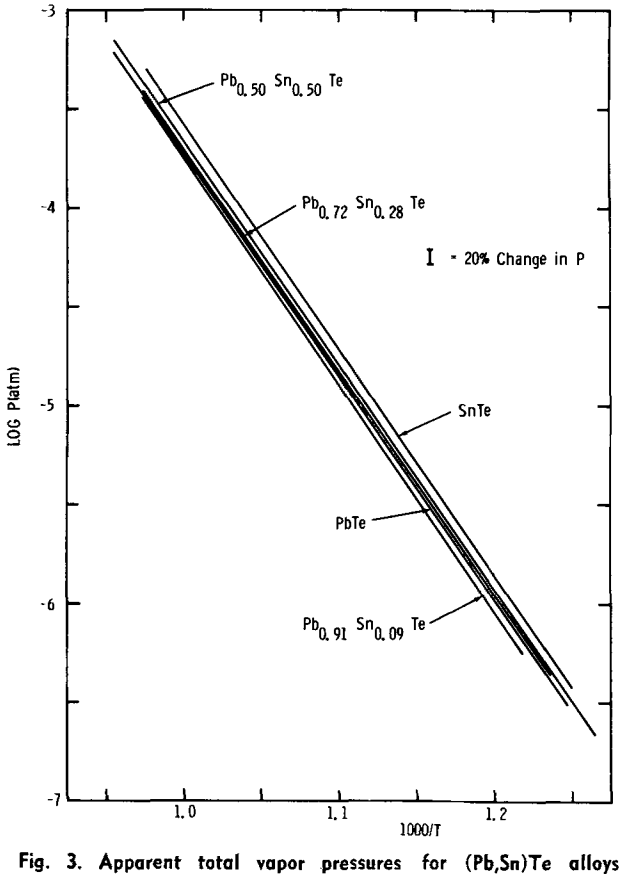

Fig. 3. Apparent total vapor pressures for (Pb,Sn)Te alloys calculated with the assumptions described in detail in the text. The over-all experimental uncertainty is of the order of the error bar given.

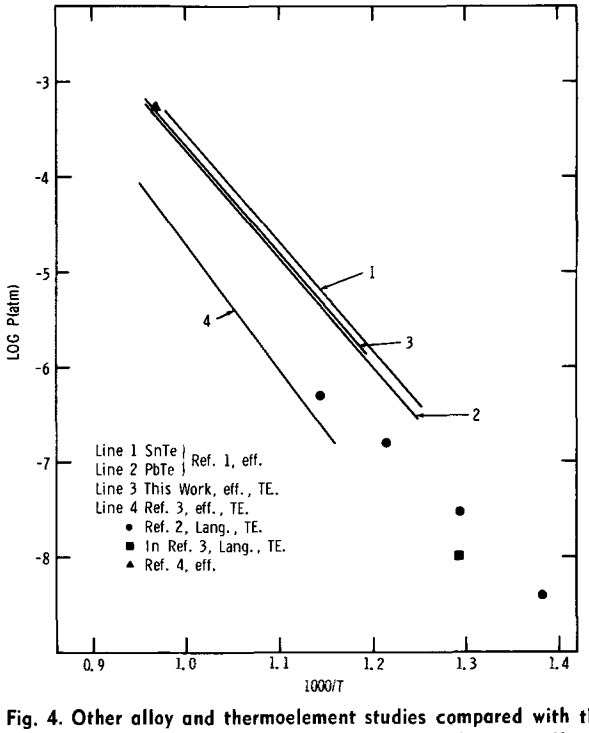

Fig. 4. Other alloy and thermoelement studies compared with the results of this study: TE = commercial thermoelement; eff. = effusion method; Lang. = free surface or Langmuir method.

Manuscript submitted Nov. 16, 1970; revised manuscript received Feb. 22, 1971.

Any discussion of this paper will appear in a Discussion Section to be published in the June 1972 JOURNAL.

REFERENCES

1. D. A. Northrop, *J. Phys. Chem.*, **75**, 118 (1971).
2. H. E. Bates and M. Weinstein, *Advan. Energy Conv.*, **6**, 177 (1966).
3. P. Winchell, *Energy Conversion*, **8**, 81 (1968).
4. V. V. Sokolov, V. I. Belovsov, V. B. Shol'ts, and L. N. Sidorov, *Russ. J. Phys. Chem.*, **40**, 885 (1966).
5. J. W. Wagner and J. C. Woolley, *Mater. Res. Bull.*, **2**, 1055 (1967).
6. N. K. Abrikosov, K. A. Dvul'dina, and T. A. Danilyan, *Russ. J. Inorg. Chem.*, **3**, 1632 (1958).
7. J. W. Wagner and R. K. Willardson, *Trans. Met. Soc. AIME*, **242**, 366 (1968).
8. A. R. Calawa, T. C. Harman, M. Finn, and P. Youtz, *ibid.*, **242**, 374 (1968).
9. R. F. Bis and J. R. Dixon, *J. Appl. Phys.*, **40**, 1918 (1969).
10. A. M. Reti, A. K. Jena, and M. B. Bever, *Trans. Met. Soc. AIME*, **242**, 371 (1968).
11. R. Mazelsky, M. S. Lubell, and W. E. Kramer, *J. Chem. Phys.*, **37**, 45 (1962).
12. N. R. Short, *Brit. J. Appl. Phys. (J. Phys. D)*, **1**, 129 (1968).
13. J. F. Butler and T. C. Harman, *This Journal*, **116**, 260 (1969).
14. A. A. Machonis and I. B. Cadoff, *Trans. Met. Soc. AIME*, **230**, 333 (1964).
15. R. N. Tauber and I. B. Cadoff, *J. Appl. Phys.*, **38**, 3714 (1967).
16. K. J. Kinden and C. A. Kennedy, *ibid.*, **40**, 2595 (1969).
17. K. Motzfeldt, *J. Phys. Chem.*, **59**, 139 (1955).
18. E. M. Levin, H. F. McMurdie, and F. P. Hall, "Phase Diagrams for Ceramists," p. 12, American Ceramic Society, Columbus, Ohio (1956).

Technical Notes

Formation of 20-25Å Thermal Oxide Films on Silicon at 950°-1140°C

J. A. Aboaf*

IBM Components Division, East Fishkill Facility, Hopewell Junction, New York 12533

Recent papers on MNOS (metal-Si_3N_4-SiO_2-Si) memory transistors, in which charge can be stored at or near the interface between the two insulators (1-6), classify them as either Fowler-Nordheim devices or direct tunneling devices, the only difference being that the latter have thinner oxide layers. For oxide layer thicknesses up to 37Å (3), the interface traps are charged by direct tunneling through the SiO_2 layer. Direct tunneling devices consequently exhibit great sensitivity of the so-called "write" characteristics to the oxide layer thickness (4, 7). Since the growth rate of SiO_2 on silicon is relatively high in oxygen or water vapor ambients (8) at high temperatures, low temperatures and/or diluted oxygen atmospheres should be used when very thin (about 20Å) films are necessary. While Wallmark and Scott (3), in their MNOS studies, prepared SiO_2 films in steam at 600°C, the present paper shows that very thin films of SiO_2 (less than 50Å) can be formed on silicon in ambient mixtures of NO and H_2 at 950°-1140°C.

P-type silicon wafers (<100>, 10 ohm-cm) were first cleaned in ammonia, hydrochloric acid, hydrofluoric acid, and deionized water, and then blown dry in nitrogen. The residual SiO_2 covering the wafers was then measured by ellipsometry (9, 10) and found to be 10 ± 1Å. The reactions were carried out using rf induction heating of a conventional horizontal quartz tube (59 mm in diameter) with a graphite susceptor encased in a fused silica envelope and attached to the cap of the reactor. High-purity hydrogen and nitric oxide gases (Matheson Corporation) were used without further purification.

The growth of oxide on these silicon wafers at 1000°C in various gas ambients is shown in Fig. 1. The oxide thickness, measured by ellipsometry, increased linearly above 25Å but probably logarithmically below 25Å.

The oxidation of Si by NO (curve A) probably occurs by the reaction of silicon with the oxygen formed while the NO gas is decomposing. The mechanism of thermal decomposition of NO in nitrogen and

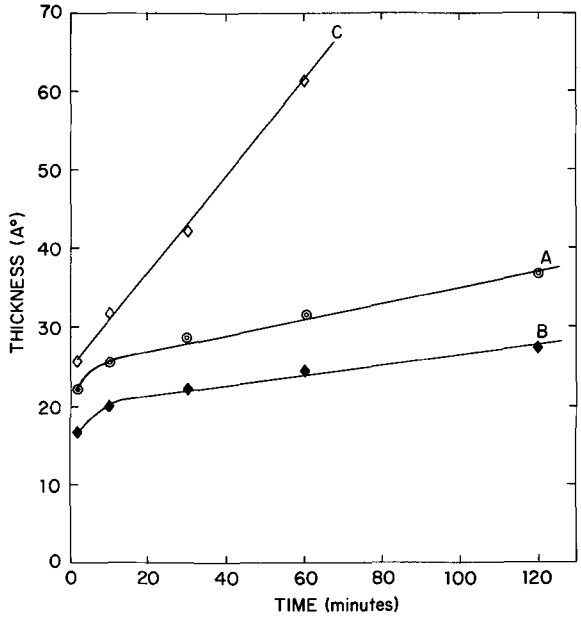

Fig. 1. Oxide growth as a function of time at 1000°C in the following gas ambients: A—6%NO, 94% N_2 in volume (total flow: 4.5 liters/min); B—6% NO, 94% H_2 in volume (total flow: 4.5 liters/min); C—0.3% O_2, 99.7% N_2 in volume.

* Electrochemical Society Active Member.

Key words: oxidation, silicon, thin films.